Neuron, Vol. 17, 979–990, November, 1996, Copyright ©1996 by Cell Press

# Identification of the Amino Acid Subsets Accounting for the Ligand Binding Specificity of a Glutamate Receptor

**Yoav Paas,* Miriam Eisenstein,† François Medevielle,‡ Vivian I. Teichberg,* and Anne Devillers-Thiéry‡**
*Department of Neurobiology
†Department of Chemical Services
The Weizmann Institute of Science
76100 Rehovot
Israel
‡Neurobiologie Moléculaire
Unité de Recherche Associée D1284
Centre National de la Recherche Scientifique
Institut Pasteur
25 rue du Dr. Roux
75015 Paris
France

## Summary

**In a situation so far unique among neurotransmitter receptors, glutamate receptors share amino acid sequence similarities with the bacterial periplasmic binding proteins (PBPs). On the basis of the primary structure similarity of two bacterial periplasmic proteins (lysine/arginine/ornithine- and phosphate-binding proteins) with the chick cerebellar kainate-binding protein (KBP), a member of the ionotropic glutamate receptor family, we have generated a three-dimensional model structure of the KBP extracellular domain. By an interplay between homology modeling and site-directed mutagenesis, we have investigated the kainate binding properties of 55 different mutants (corresponding to 43 positions) and studied the interactions of some of these mutants with various glutamatergic ligands. As a result, we present here the subsets of amino acids accounting for the binding free energies and specificities of KBP for kainate, glutamate, and CNQX and propose a three-dimensional model, at the microarchitectural level, of the glutamatergic binding domain.**

## Introduction

The membrane receptors mediating the effects of the excitatory neurotransmitter glutamate (Glu) in the vertebrate central nervous system have been the subject, in recent years, of extensive research aimed at the characterization of their structure and function. Molecular cloning of a large number of Glu receptors has established that they belong to two protein subfamilies distinguishable by the presence of either seven or four putative transmembrane (TM) domains. The metabotropic Glu receptors (mGluRs) that act via G proteins belong to the TM7 receptor subfamily (Pin and Duvoisin, 1995). The other receptor subfamily includes the ionotropic Glu receptors (iGluRs) that function as ligand-gated channels (reviewed by Gasic and Hollmann, 1992; Hollmann and Heinemann, 1994) and the various kainate-binding proteins (KBPs) (Gregor et al., 1989; Wada et al., 1989; Wo and Oswald, 1994), which are all supposed to harbor three membrane-spanning segments (TMI, TMIII, and TMIV) and one membrane-embedded domain (MII) (Hollmann et al., 1994; Wo and Oswald, 1994, 1995; Bennett and Dingledine, 1995).

Detailed amino acid sequence comparisons between bacterial periplasmic binding proteins (PBPs) and mGluRs together with site-directed mutagenesis studies have established that the amino-terminal domain (ATD) of mGluRs forms a functional agonist-binding site with a three-dimensional (3D) structure analogous to that of the leucine/isoleucine/valine-binding protein (LIVBP) (O'Hara et al., 1993). The PBPs are soluble proteins involved in the recognition and transport into the cell of amino acids, saccharides, vitamins, and inorganic ions (Ames, 1986) and which possess similar 3D structures (Quiocho, 1990; Kang et al. 1991; Oh et al., 1993, 1994) in spite of the fact that their amino acid sequences may share no similarity.

Amino acid sequence alignments (Nakanishi et al., 1990; O'Hara et al., 1993) of iGluRs with PBPs have suggested that the iGluRs are composed of two modules of PBPs, a LIVBP-like module at the amino terminus, followed by a glutamine-binding protein (QBP) / lysine/arginine/ornithine-binding protein (LAOBP)-like module split into two domains S1 and S2 (nomenclature of Stern-Bach et al., 1994) separated by the first three putative membrane-embedded segments. Since the PBPs are all composed of two lobes with the ligand-binding site located in the interlobe cleft, it was proposed that the two regions S1 and S2 of the QBP/LAOBP-like module of iGluRs are spatially organized like the PBPs creating a specific ligand-binding site at their interface. Although support for this spatial organization was obtained from several studies (Kuryatov et al., 1994; Stern-Bach et al., 1994; Kuusinen et al., 1995), the specific amino acid residues lining the Glu-binding pocket have not been identified so far. Thus, an understanding of the microarchitectural motifs creating the ligand subtype specificity of these Glu receptors is still missing.

To establish the structural basis of the pharmacological specificity of a member of the family of the kainate (KA) subtype of Glu receptors, we undertook a detailed investigation of the ligand-binding domain of the chick cerebellar KBP. This choice was motivated by the following facts: KBP is a protein with half the size of KA receptors, but with the very same pharmacological properties (Gregor et al., 1988); KBP possesses various mutually exclusive ligands that are likely to share a common binding site (Gregor et al., 1988; Gorodinsky et al., 1993); and a DGKYG (residues 70–74) sequence, which is part of a GxGxxG consensus nucleotide-binding motif (Hanks et al., 1988; Branden and Tooze, 1991; Bourne et al., 1991), has already been identified as forming part of the ligand-binding site of KBP (Paas and Teichberg, 1992; Paas et al., 1994), and the role of residue Y73 in KA and GTP binding has been established (Paas et al., 1996).

Performing ligand binding measurements on 55 KBP mutants selected on the basis of the established structural similarity of Glu receptors with PBPs, we have now identified the subsets of amino acid residues forming, respectively, the KA, Glu, and 6-cyano-7-nitroquinoxaline-2,3-dione (CNQX) subsites within the ligand-binding domain

of KBP. On the strength of these data, we propose here a 3D model structure of the KBP ligand-binding domain that fully accounts for the selectivity, competitive interactions, and binding energetics of the above mentioned KBP ligands. This model can now serve as a template for the elaboration of parallel models of the ligand-binding domain of all Glu receptor channels.

## Results

### Probing the KBP Putative Ligand-Binding Domain

To guide the selection of the KBP ligand-binding amino acids to be mutated, we initially built a 3D model structure based both on the X-ray structure of LAOBP (Oh et al., 1993) and on the amino acid sequence alignment of KBP with LAOBP as proposed by O'Hara et al. (1993). We then mutated by site-directed mutagenesis the amino acid residues aligning with the ligand-binding residues of LAOBP. We also mutated the residues located in the interlobe cleft (i.e., in the putative ligand-binding pocket) and in its vicinity. Furthermore, we mutated residues in the glycine-rich motif (G69–G74, which include the GxGxxG nucleotide-binding motif) as well as those amino acids present in the KBP segment W82–Q92 that has no counterpart in LAOBP according to O'Hara et al. (1993). Finally, we mutated residues in segment K276–K297 that do not align well with LAOBP. In most cases, residues were substituted with alanine, but specific amino acid substitutions were also made to produce more limited reductions of either charge, hydrogen bonding capacity, or bulkiness.

Following transfection of human embryonic kidney (HEK) 293 cells with the various plasmids harboring the mutated KBP cDNAs, we carried out measurements of the displacement by unlabeled KA of [$^3$H]KA bound to purified membrane preparations and determined the values of the apparent dissociation constant for inhibition, $Ki_{(KA)}$, for all mutants. For the mutants found to affect KA binding, the respective $\Delta G^\circ$ values were then calculated from the relation: $\Delta G^\circ = -RT\ \ln Ki_{app}$.

The $\Delta G^\circ$ values of the Gibbs free energy of binding were used in the following way to help us in the assessment of whether all the amino acids that contribute to the binding of a given ligand have been identified. Assuming that the mutation does not modify the conformation of the ligand-binding domain, we reasoned here that a mutation in the binding site will primarily affect the ability of the replacing residue to interact directly with the ligand, but may also perturb the short distance interactions made upon ligand binding by the given residue with its neighbors. By subtracting the value $\Delta G^\circ$ measured for the mutant from that obtained for wild-type (WT) KBP, a value $\Delta\Delta G^\circ$ is obtained. The latter represents the contribution of the substituted side chain to the ligand binding energy. It will be underestimated if the replacing residue at the mutated position contributes, by itself, to the ligand binding free energy. It will be overestimated if the substituting residue itself, while not being in direct contact with the ligand, weakens binding by affecting its neighbors in the ligand-binding pocket. Adding the $\Delta\Delta G^\circ$ values for all the mutations affecting the binding of a given ligand, one obtains a value designated as $\Sigma\Delta\Delta G^\circ$. A condition in which $\Sigma\Delta\Delta G^\circ < \Delta G^\circ_{(WT)}$ clearly indicates that not all the residues contributing to the binding have been identified, while a $\Sigma\Delta\Delta G^\circ$ value higher than the $\Delta G^\circ_{(WT)}$ suggests that the interactions made by the residues contributing to the $\Sigma\Delta\Delta G^\circ$ value are necessary and possibly sufficient to account for the ligand binding energetics. However, it is clearly possible that additional residues are involved or that some residues interact only indirectly with the ligand and contribute to binding by stabilization of the ligand-binding pocket via a hydrogen bond network (Berland et al., 1995) or via the solvent.

Using this approach, we observed that the mutations found to reduce the affinity for KA (E33V, Y36F, Y73I, and T102A) did not fully account for KA binding free energy. Moreover, the substitution of the other amino acids that align with the ligand-binding residues of LAOBP (O'Hara et al., 1993) and that were predicted to contribute to KA binding were found either to not affect KA binding (T30A and L263A) or to completely abolish it (R107S, T268A, and E316A/Q). In the latter case, the transfected cell membrane preparations were also submitted to SDS–polyacrylamide gel electrophoresis (SDS–PAGE) to allow the probing, with anti-KBP antibodies, of the presence and integrity of KBP (see below).

On the strength of these results and assuming that R107, T268, and E316 were not involved in ligand binding, we reasoned that the reliance on the LAOBP template for KBP modeling had to be challenged. In the search for an alternative and guided by the approach described in detail in the Experimental Procedures (under the heading Alignments and Computer-Assisted Molecular Modeling), we observed that the atomic coordinates of two PBPs, the LAOBP (Oh et al., 1993) and the phosphate-binding protein (PhosBP; Luecke and Quiocho, 1990; Wang et al., 1994), were likely to provide more appropriate templates for building a model structure of KBP. This model structure includes two lobes, I and II, built according to the atomic coordinates of LAOBP and PhosBP, respectively. It also suggests a novel sequence alignment between KBP and PBPs (Figure 1) that differs from the three alignments proposed (Nakanishi et al., 1990; Cockcroft et al., 1993; O'Hara et al., 1993). Upon inspection of the interlobe cleft of this KBP hybrid model structure, several predictions were made. Accordingly, we performed a second round of mutations and observed that, indeed as expected, mutants displaying the substitutions S266A, S267A, and Y299A exhibited a decreased affinity toward KA.

In Table 1, we present the KA binding parameters of all the KBP mutants. Calculating the $\Sigma\Delta\Delta G^\circ$ value for the set of mutations displaying a reduced affinity for KA (see Table 3), one observes that it is in excess of the $\Delta G^\circ$ for WT KBP. Thus, on the basis of this criterion, we concluded that most if not all the amino acids involved in KA binding have been identified. Since the predictions of the KBP hybrid model turned out to be correct for KA binding, we used it as well for the identification of the subset of amino acids accounting for the binding of Glu and CNQX (Table 2), focusing mainly on the mutations displaying a reduced KA affinity.

### Identification of the Amino Acids Lining the Ligand-Binding Pocket

On the basis of the results obtained from 55 mutants corresponding to 43 different locations, four classes of

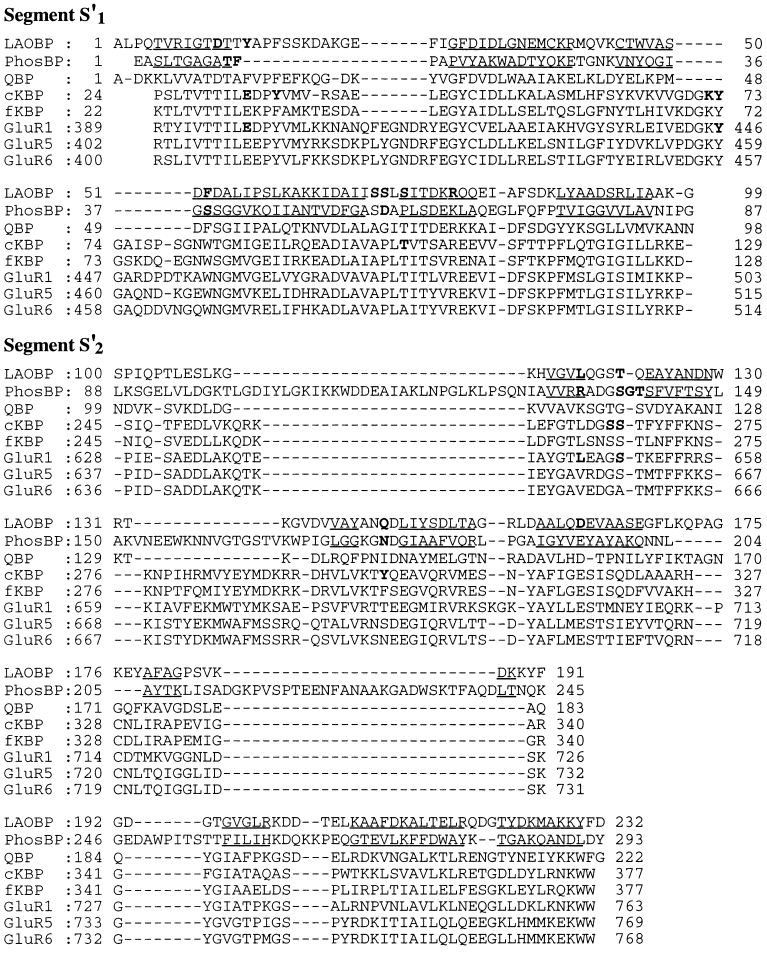


Figure 1. Multiple Alignment of Bacterial PBPs with Selected KBPs and iGluRs

The sequences of LAOBP and PhosBP were taken from X-ray structures (Oh et al., 1993; Luecke and Quiocho, 1990). For definition of segments $S'_1$ and $S'_2$, see legend to Figures 4A and 4B. cKBP and fKBP correspond to proteins from chick cerebellum and frog brain, respectively. LAOBP and PhosBP cannot be aligned by standard alignment programs and were therefore aligned on the basis of their X-ray structures. The structural alignment was performed separately for lobe I (LAOBP residues 1–88 plus 196–232) and lobe II (LAOBP residues 89–195) by superimposing the Cα atoms of corresponding secondary structure elements that are denoted here by the underlined residues. The root square mean deviation (rsmd) for 84 Cα atoms in the upper lobe is 2.9 Å, and the rsmd for 47 Cα atoms in the lower lobe is 2.5 Å. The alignment of cKBP with LAOBP and PhosBP was carried out as described in the Experimental Procedures. QBP, fKBP, GluR1, GluR5, and GluR6 were aligned with KBP using FASTA. Except for the PhosBP N177 and LAOBP Q143 (see below), the bold residues correspond to amino acids shown to be either in contact with the ligand (LAOBP and PhosBP) or to be involved in ligand binding (cKBP, GluR1 [Paas et al., 1996; Mano et al., 1996]). The PhosBP N177 and LAOBP Q143 residues were shown to be located within the ligand-binding pocket and to contribute to its bond network via PhosBP T10 andT141 and LAOBP Y14, respectively.

mutations were defined: mutations that reduced the KBP affinity for a ligand by at least a factor of five (Figure 2; bold letters in Tables 1 and 2); mutations that caused partial or total degradation of KBP and a subsequent loss of KA binding (Figure 3 and Table 1); mutations that caused no degradation of KBP but a complete loss of KA binding (Figure 3 and Table 1); mutations that produced no changes in the KBP affinity for KA, Glu, or CNQX (Tables 1 and 2).

### *Mutations That Significantly Reduced the KBP Affinity for at Least One Ligand*

Tables 1 and 2 and Figure 2 show that only eight amino acid residues of the 43 positions examined are involved in ligand binding: E33, Y36, Y73, P100, T102, S266, S267, and Y299. Their involvement is ligand selective as expected from residues forming a binding pocket able to recognize ligands with very different chemical structures. The sets of amino acids involved in binding not only differ for each ligand, but also in the extent of their involvement. Substitution of E33 for valine exerts a very strong effect (110-fold decrease) solely on KA binding. In contrast, the decrease in binding affinity for Glu is much more profound than for KA in the case of Y36F (30- and 5-fold, respectively), Y73I (90- and 10-fold, respectively), and T102A (100- and 58-fold, respectively). The moderate but statistically very significant effect on the KA binding affinity revealed in the case of S266A, S267A, and Y299A (5- to 6-fold decrease) is not observed for Glu binding. CNQX binding is affected only by the mutation of one of the amino acids involved in the binding of KA and Glu. Indeed, Y73 appears to play a pivotal role in ligand recognition as it is involved in the binding not only of all three ligands, but also of GTP (Paas et al., 1996). In contrast, replacement of P100 for an alanine resulted in a significant loss of binding affinity for CNQX, a small effect on Glu binding, and no effect on KA binding.

According to the results presented in Table 3, the amino acid residues forming the KA- and Glu-binding sites seem to have been identified, but not all those forming the CNQX-binding site. In the latter case, we investigated all the KBP mutants harboring mutations of residues predicted to be in the ligand-binding pocket and displaying KA binding. This included mutations of W82, L101, and T30 located in the vicinity of the interlobe cleft. Although the apparent Ki value for CNQX could not be determined from the displacement curve observed for Y73I (Figure 2 and Table 2), the contribution of this tyrosine side chain to the CNQX binding free energy can be estimated to be larger than 4 kcal/mol.

Inspection of the data presented in Figure 2 and Table 1 shows that the displacement curves for KA binding display Hill coefficient ($n_H$) values significantly greater than 1.0 but smaller than 2.0, indicating that KA binds, in a cooperative manner, to two subunits of the membranous KBP complex. Interestingly, the E33V, T102A, S266A, and S267A mutants exhibit approximately the same $n_H$ values as WT KBP, while Y36F, Y73I, and Y299A

Table 1. Apparent Ki Values in μM (mean ± SD) and Hill Coefficients ($n_H$ ± SD) for KA Binding to WT KBP and Its Mutants

| Lobe I | | | Lobe II | | |
|---|---|---|---|---|---|
| Mutation | Ki Value | Hill Coefficient | Mutation | Ki Value | Hill Coefficient |
| *T30A | WT | | *L263A | WT | |
| ***E33V** | 50.6 ± 16.4 | 1.4 ± 0.1 | *L263T | WT[a] | |
| Y36A | NB | | G265N | NB | |
| Y36I | NB | | **S266A** | 2.5 ± 0.8 | 1.4 ± 0.1 |
| **Y36F** | 2.3 ± 0.3 | 1.8 ± 0.1 | **S267A** | 2.3 ± 0.3 | 1.6 ± 0.1 |
| D70S | NB | | *T268A | NB | |
| D70N | WT[a] | | Y270F | WT | |
| K72A | WT | | V283A | WT | |
| K72T | WT | | Y284A | WT | |
| **Y73I** | 4.8 ± 0.9 | 1.9 ± 0.1 | Y284I | WT | |
| S79V | WT | | E285A | WT | |
| W82A | WT | | Y286I | WT | |
| T83A | NB | | M287A | NB | |
| G84A | NB | | M287V | WT | |
| M85A | WT | | D288A | WT | |
| I86A | WT | | D288S | WT | |
| G87R | WT | | K289S | WT | |
| E88V | WT | | R290S | WT | |
| I89A | WT | | R291S | WT | |
| L90A | NB | | V294A | NB | |
| L90V | WT | | V294I | WT[a] | |
| *P100A | WT | | L295A | WT | |
| L101A | NB | | K297T | WT | |
| L101V | WT | | **Y299A** | 2.6 ± 0.5 | 1.9 ± 0.1 |
| ***T102A** | 26.2 ± 7.7 | 1.4 ± 0.1 | *E316A | NB | |
| *R107S | NB | | *E316Q | NB | |
| | | | S317A | WT | |
| | | | F342I | NB | |
| | | | G343A | WT | |

The apparent Ki value for WT KBP is 0.45 ± 0.05 μM and its $n_H$ = 1.50 ± 0.1. Asterisks indicate the residues aligning, according to O'Hara et al. (1993), with the ligand-binding residues of LAOBP. The mutants in bold correspond to residues likely to be involved in KA binding. Their apparent KA binding affinity significantly differs from that of the WT KBP ($p < 0.015$). Y36F, Y73I, and Y299A display significantly different Hill coefficient value compared with WT KBP ($p < 0.025$). All values were rounded to the closest decimal number.

WT indicates that the mutant KBP binds the ligand with the same affinity as WT KBP or with slightly decreased apparent affinity, up to 2-fold. WT[a] represents the cases in which the apparent affinity decreased up to 3-fold.

NB represents the mutants that showed no [$^3$H]KA binding. The expressed level and integrity of the KBP mutants as probed with anti-KBP antibodies are shown in Figure 3.

mutants display significantly higher values. In allosteric proteins, a change of the $n_H$ due for instance to a mutation indicates a loss or gain of intersubunit interaction energy. In the case of two identical binding sites, the free energy of intersubunit interactions ($\Delta G^\circ_H$) can be calculated from the relation $\Delta G^\circ_H = \frac{1}{2}RT \ln[(2 - n_H)/n_H]$ (Wyman, 1964; Levitzki, 1978). Subtraction of the $\Delta G^\circ_H$ values calculated for the KBP mutants from that of WT KBP yields a $\Delta\Delta G^\circ_H$ value (see footnotes to Table 3). The latter represents the gain or loss of energy of intersubunit interactions. The $\Delta\Delta G^\circ_H$ values are small but significant and may account for part of the loss of ligand binding free energy ($\Delta\Delta G^\circ$) displayed by Y36F, Y73I, and possibly by Y299A. Notably, CNQX binding to WT KBP and its P100A mutant display no cooperativity ($n_H = 1.0$) as expected from an antagonist.

### *Mutations That Caused Partial or Total Degradation of KBP and Subsequent Loss of KA Binding*

Figure 3 presents data illustrating the finding that several mutations lead to partial or total degradation of KBP. These include Y36A, D70S, T83A, G84A, L90A, L101A, G265N, M287A, and E316A. However, when more conservative mutations are made at some of these positions (D70N, L90V, L101V, and M287V), no degradation takes place, and the mutated KBP binds ligands with approximately the same affinity as the WT KBP (Figure 3 and Table 1).

### *Mutations That Caused No Degradation of KBP but a Complete Loss of KA Binding*

The pattern of migration on SDS–polyacrylamide gels of the Y36I, R107S, T268A, V294A, E316Q, and F342I mutants is also presented in Figure 3 because they belong to a group of mutants that migrate as the WT KBP, but display no detectable KA binding affinity (see Table 1). This lack of binding is not due to a low level of expression of the mutated proteins. The intensity of the immunolabeling of the KBP mutants is equal to or stronger than that of WT KBP (Figure 3). Therefore, one cannot conclude as to the role in ligand binding of the residues R107, T268, E316, and F342 though, as described below, they are located in the vicinity of the predicted ligand-binding pocket.

### *Mutations That Produced No Significant Changes in KBP Affinity for KA, Glu, and CNQX*

Of the 43 different locations at which amino acid substitution were made, 29 had no influence on ligand binding. Mutations as drastic as G87R, E88V, or E285A did not affect KA, Glu, or CNQX binding, indicating that the

Table 2. Apparent Ki Values (mean ± SD) and Hill Coefficients ($n_H$ ± SD) for Glu and CNQX Binding to WT KBP and Its Mutants Carrying Mutations of Residues Located in the Predicted KA-Binding Pocket and Its Vicinity

| KBP Mutant (or WT) | Glu (μM) | $n_H$ | CNQX (μM) | $n_H$ |
|---|---|---|---|---|
| WT KBP | 30 ± 3 | 1.2 ± 0.1 | 0.8 ± 0.1 | 1.0 ± 0.1 |
| *T30A | WT | | WT | |
| *E33V | WT | | WT | |
| **Y36F** | 924 ± 155 | 1.8 ± 0.1 | WT | |
| **Y73I** | 2694 ± 713 | 1.8 ± 0.1 | NC | |
| W82A | WT[a] | | WT[a] | |
| ***P100A** | WT[a] | | 8.0 ± 2.3 | 1.0 ± 0.1 |
| L101V | WT | | WT | |
| ***T102A** | 3060 ± 1167 | 1.0 ± 0.1 | WT | |
| S266A | WT | | WT | |
| S267A | WT | | WT | |
| Y299A | WT | | WT | |

The mutants in bold correspond to residues likely to be involved in Glu or CNQX binding. Their Glu or CNQX binding affinity is significantly different from that of WT KBP ($p < 0.015$). Y36F and Y73I display significantly different $n_H$ values compared with WT KBP ($p < 0.002$). All values were rounded to the closest decimal number.

Asterisks, WT, and WT[a] are as in Table 1.

NC indicates that the apparent Ki value could not be calculated because of the lack of CNQX solubility at concentrations ≥0.5 mM (see Figure 2C).

disruption of local networks of interactions did not cause distant detrimental effects.

## Discussion

The notion according to which the ATD and the TMIII–TMIV-connecting segment of iGluRs form an extracellular ligand-binding domain shaped like the bilobated bacterial PBPs (O'Hara et al., 1993) has already been supported by studies showing that both segments contribute to the pharmacological specificities of iGluRs (Kuryatov et al., 1994; Stern-Bach et al., 1994; Kuusinen et al., 1995; Hirai et al., 1996). However, no description of the ligand-binding pocket of a Glu receptor was made until now to account in detail for its pharmacological specificities. In the present study, we have identified, in the chick cerebellar KA-binding protein, a member of the KA/AMPA (α-amino-3-hydroxy-5-methyl-4-isoxazole-propionic acid) receptor family, the amino acid residues forming the sites of interactions of KA, Glu, and CNQX. This identification was rendered possible by the methodology adopted here that combines site-directed mutagenesis, ligand binding measurements, free energy determinations, and computer-assisted molecular modeling.

Previous studies on non-NMDA (N-methyl-D-aspartate) receptors have used only some of the components of this methodology and, thus, did not reach the present level of resolution. Uchino et al. (1992), Li et al. (1995), and Mano et al. (1996) have mutated residues in the putative extracellular portions of AMPA receptors and, by using electrophysiological recordings from Xenopus oocytes, observed changes in the agonist efficacy of Glu, AMPA, and quisqualate (Quis) but not of KA. Whether the mutations affected ligand binding rather than the channel activation pathway could not be unequivocally distinguished. However, in Mano et al. (1996), the residues affecting the ability of Quis and Glu to inhibit KA-evoked currents align with the ligand-binding residues of LAOBP. Stern-Bach et al. (1994) performed electrophysiological recordings and ligand binding measurements on KA/AMPA receptor chimeras and provided an elegant demonstration that the S1 and S2 segments determine the pharmacological specificities of iGluRs. However, this study as well as that of Kuusinen et al. (1995), who produced a soluble Glu/AMPA-binding domain, did not shed light on the specific amino acids directly involved in binding of Glu, KA, or AMPA.

Kuryatov et al. (1994), Wafford et al. (1995), and Hirai et al. (1996) also used the methodology of site-directed mutagenesis followed by electrophysiological recordings to reveal the amino acids of the NMDA R1 subunit involved in glycine and/or Glu activation. The mutated residues affecting the efficacy of glycine as a coagonist were found to be at positions equivalent to those forming the ligand-binding site of LAOBP. It remains possible, however, that some mutations produced allosteric effects, since the response properties of Glu were also affected, albeit to a lesser extent. Thus, not all the identified amino acids may directly interact with glycine. In this respect, inspection of the KBP hybrid model structure suggests that a small ligand such as glycine is unlikely to be in concurrent contact with all the residues suggested by Kuryatov et al. (1994) and Hirai et al. (1996).

It is of importance to point out that the results of ligand binding measurements performed in the present study on mutant receptor proteins at equilibrium, and the subsequent calculations of the binding free energies and their sums ($\Sigma\Delta\Delta G^\circ$), are not on their own devoid of ambiguities of interpretation. The reasons for this are as follows: a mutation of a ligand-binding residue may affect the network of mutual interactions between residues in the ligand-binding pocket (Schreiber and Fersht, 1995) and may subsequently affect ligand binding indirectly as well; the substituting side chain might weaken ligand binding, while not being in direct contact with the ligand; mutations affecting the ligand-binding residues cannot be readily distinguished from those of residues involved in the maintenance of the conformation of the entire ligand-binding domain. These various side effects (mentioned above) may cause the $\Sigma\Delta\Delta G^\circ$ to exceed significantly the $\Delta G^\circ$ value of KA binding to WT KBP. Thus, the $\Sigma\Delta\Delta G^\circ$ value should be seen only as an assisting tool. It cannot be used exclusively to decide on the nature and number of amino acid residues involved in binding. Information on the high affinity desensitized state of the receptor is obtained when ligand binding studies are performed at equilibrium. Thus, only amino acids contributing to high affinity ligand binding may be identified, while those involved exclusively in the low affinity active state may not be identified.

The ambiguities of mutagenesis followed by ligand binding studies are nevertheless counterbalanced in the present case by the availability of the already resolved protein structures of LAOBP and PhosBP that can be used as templates for KBP model building. Accordingly, the proposed model structure can be examined to determine whether the amino acids identified as forming a specific ligand-binding site are found at spatial locations compatible with the chemical structure and space-filling properties of the ligand. Although a model structure

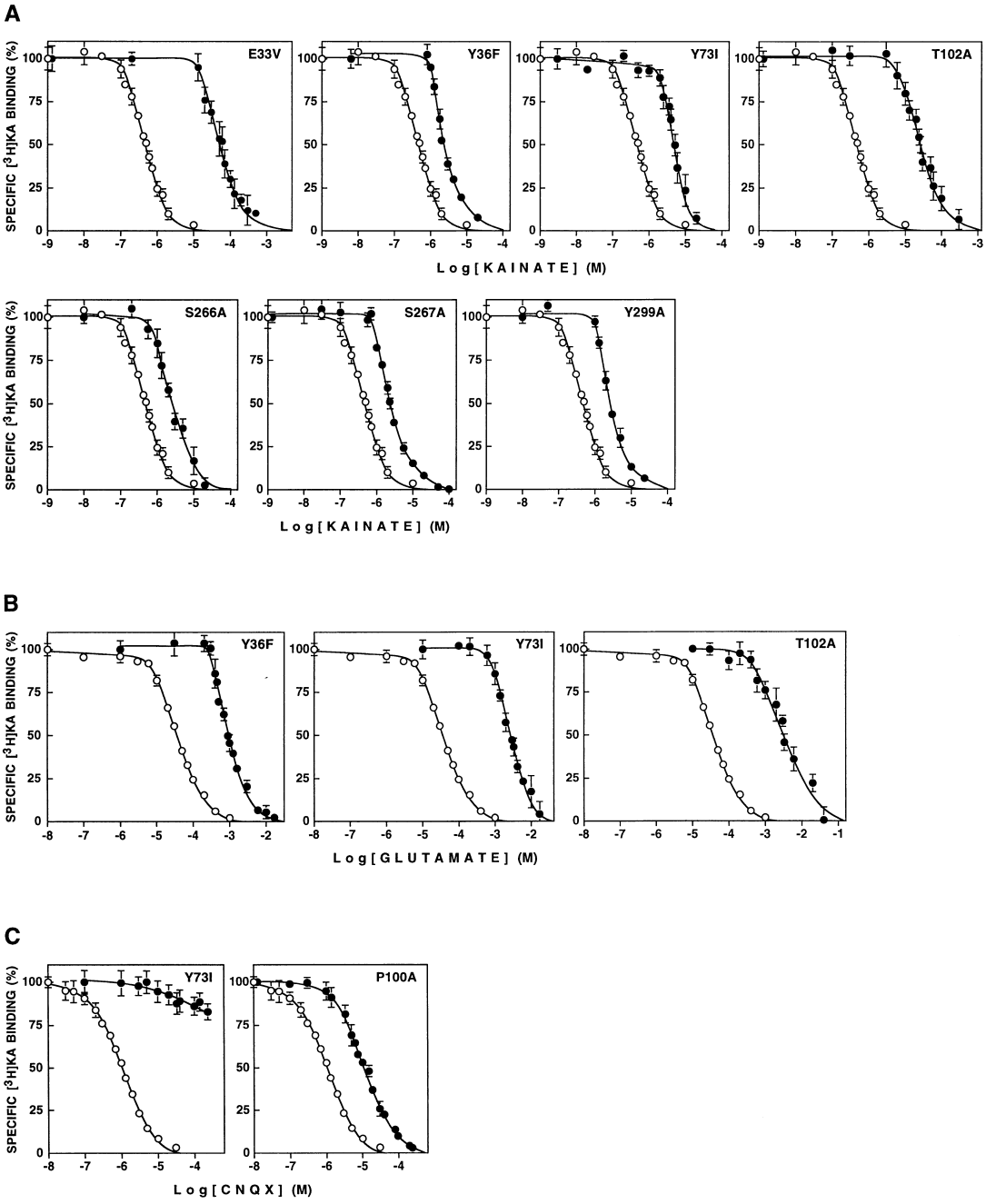


Figure 2. Mutations Affecting Ligand Binding to KBP

Inhibition of the binding of [$^3$H]KA to membrane-bound WT KBP (open circles) and its mutants (closed circles) by KA (A), Glu (B), and CNQX (C). The substituted amino acids, their positions, and the replacing residues are indicated within the small figures. Error bars represent the standard deviation for at least two experiments performed in triplicates. The binding parameters are detailed in Tables 1 and 2.

remains only an approximation of the real structure, it is of heuristic value if the suggested structure is coherent and in agreement with the experimental results.

### The Ligand-Binding Pocket

The boundaries of the ligand-binding pocket are defined, from a biochemical point of view, by the amino acid residues for which mutations affect ligand binding. They are also delineated, on the basis of the KBP model, by the location outside the interlobe cleft, of the many residues that were found not to be involved in ligand binding (green balls in Figure 4; see below). Inspection of the results presented in Figure 2 and Tables 1–3 readily reveal that the residues involved in ligand binding are mainly those that were predicted to be in the ligand-binding pocket from both the sequence similarity between KBP and bacterial PBPs (see Figure 1) and from the model structure based on the established X-ray

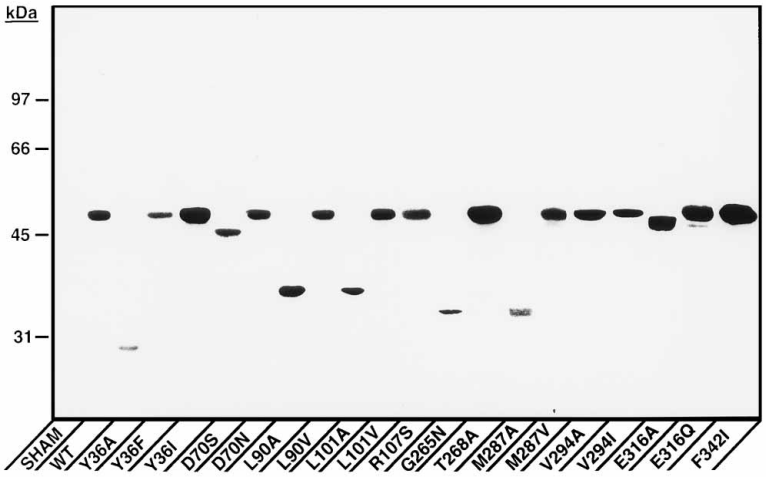


Figure 3. Immunoblot of Membrane-Bound WT KBP and a Few of Its Mutants

HEK 293 cells were transfected with an empty pMT3 plasmid (sham) or with a pMT3 plasmid harboring cDNAs encoding WT KBP or its mutants. Following membrane preparation, aliquots of 40 μg proteins were subjected to analysis by SDS–PAGE followed by immunoblotting with affinity-purified polyclonal anti-KBP antibodies. The WT KBP is seen as a 49 kDa polypeptide and corresponds to a preparation expressing 300 pmol KBP/mg protein. Note that the crude membrane preparations possibly contain ER- and Golgi membrane-bound KBP. However, when WT KBP or its mutants that display the same KA binding affinity were expressed, there was a linear correlation between the ECL signal and the level of [$^3$H]KA binding. The substituted amino acids, their positions, and the replacing residues are indicated within the figure. The KBP mutants T83A and G84A with which several transfections were made were not detected by the specific antibodies. We assume that the T83A and G84A mutants underwent complete degradation, since the cells transfected with these two mutants displayed the typical morphological changes of high KBP expression (round and poorly adhering cells).

structures of two PBPs (Figure 4). Particularly in lobe I, the ligand-binding residues of KBP share with those of bacterial PBPs similar side chain properties. In all iGluR subunits, the aromaticity at positions equivalent to the Glu/KA-binding residues of KBP, Y36, and Y73 is conserved. The same applies to the hydroxyl moiety of T102, except in the case of GluR6, that harbors an alanine at the equivalent position. E33 that was shown, upon mutagenesis, to affect KA but not Glu binding affinity is conserved in all non-NMDA receptors. S267 is conserved in most of the iGluRs. The KBP ligand-binding pocket includes Y299, which is not conserved. It is noteworthy that the AMPA and KA ionotropic receptors contain, at the equivalent position, a hydroxyl moiety. In addition, Y299 aligns with the PhosBP N177 residue that is located within the phosphate-binding pocket and contributes to the bond network that stabilizes it. None of the ligand-binding residues is positively charged, but all of them, except for P100, have the ability to form hydrogen bonds. Such a mode of ligand binding, based on hydrogen bonding rather than ionic pairing, is surprising in view of the fact that KBP binds preferentially dicarboxylic amino acids such as KA, domoate, and Glu.

### Amino Acids Likely to Contribute to the Stabilization of the Tertiary Structure

The KBP hybrid model structure places the side chains of R107, T268, E316, and F342 in the vicinity of the

Table 3. Ligand Binding Energetics of WT KBP and Its Mutants

| | KA | | | Glu | | | CNQX | |
|---|---|---|---|---|---|---|---|---|
| KBP WT or Mutant | $\Delta G^\circ$ | $\Delta\Delta G^\circ$ | $\Delta\Delta G^{\circ\prime}$ | $\Delta G^\circ$ | $\Delta\Delta G^\circ$ | $\Delta\Delta G^{\circ\prime}$ | $\Delta G^\circ$ | $\Delta\Delta G^\circ$ |
| E33V | 5.4 ± 0.2 | 2.6 ± 0.2 | 2.7 ± 0.2 | WT | 0 | 0 | WT | 0 |
| Y36F | 7.1 ± 0.1 | 0.9 ± 0.1 | 0.6 ± 0.2[a] | 3.8 ± 0.1 | 1.9 ± 0.1 | 1.3 ± 0.2[b] | WT | 0 |
| Y73I | 6.7 ± 0.1 | 1.3 ± 0.1 | 0.7 ± 0.3[a] | 3.2 ± 0.2 | 2.5 ± 0.2 | 2.0 ± 0.2[a] | NC | NC |
| P100A | WT | 0 | 0 | WT | 0 | 0 | 6.5 ± 0.2 | 1.2 ± 0.2 |
| T102A | 5.8 ± 0.2 | 2.2 ± 0.2 | 2.3 ± 0.2 | 3.2 ± 0.3 | 2.5 ± 0.3 | 2.6 ± 0.3 | WT | 0 |
| S266A | 7.1 ± 0.2 | 0.9 ± 0.2 | 1.0 ± 0.2 | WT | 0 | 0 | WT | 0 |
| S267A | 7.1 ± 0.1 | 0.9 ± 0.1 | 0.8 ± 0.1 | WT | 0 | 0 | WT | 0 |
| Y299A | 7.1 ± 0.1 | 0.9 ± 0.1 | 0.6 ± 0.3[c] | WT | 0 | 0 | WT | 0 |
| WT KBP | 8.0 ± 0.1 | 0 | 0 | 5.7 ± 0.1 | 0 | 0 | 7.7 ± 0.1 | 0 |
| $\Sigma\Delta\Delta G^\circ$ | | 9.7 ± 0.4 | | | 6.9 ± 0.4 | | | NC |
| $\Sigma\Delta\Delta G^{\circ\prime}$ | | | 8.7 ± 0.6 | | | 5.9 ± 0.4 | | |

WT and NC are as in Table 2.

Gibbs free energies $\Delta G^\circ$ in kcal/mol, are calculated as described in Experimental Procedures.

$\Delta\Delta G^\circ = \Delta G^\circ_{(WT)} - \Delta G^\circ_{(mut)}$.

The calculated $\Delta\Delta G^{\circ\prime}$ value is the net free energy of binding and accounts for the fact that $\Delta\Delta G^\circ$ includes the gain or loss of energy of intersubunit interactions ($\Delta\Delta G^\circ_H$). Thus, $\Delta\Delta G^{\circ\prime} = \Delta\Delta G^\circ - \Delta\Delta G^\circ_H$ where $\Delta\Delta G^\circ_H = \Delta G^\circ_{H(WT)} - \Delta G^\circ_{H(mut)}$ and $\Delta G^\circ_H = +0.5\ RT\ \ln[(2-n_H)/n_H]$, $n_H$ being the Hill coefficient value. For example, for WT KBP, $n_H = 1.5$, thus, $\Delta G^\circ_{H(WT)} = 0.5 \times RT \times \ln[(2-1.5)/1.5] = -0.3$ kcal/mol. The negative value indicates that energy ought to be invested to allow the intersubunit allosteric transition. For Y73I, the intersubunit interaction energy is $\Delta G^\circ_{H(Y73I)} = 0.5 \times RT \times \ln[(2-1.93)/1.93] = -0.9$ kcal/mol, thus $\Delta\Delta G^\circ_{H(Y73I)} = -0.3$ kcal/mol $- -0.9$ kcal mol $= +0.6$ kcal/mol. $\Delta\Delta G^{\circ\prime}_{(Y73I)} = 1.3$ kcal/mol $- 0.6$ kcal/mol $= 0.7$ kcal/mol.

All values were rounded to the closest decimal number. However, the nonrounded figures were used for the statistical analysis. $\Delta G^\circ_{(mut)}$ versus $\Delta G^\circ_{(WT)}$: $p < 0.0015$. $\Delta\Delta G^\circ$ versus $\Delta\Delta G^{\circ\prime}$: [a] $p < 0.05$; [b] $p < 0.01$; and [c] $p < 0.11$. $\Sigma\Delta\Delta G^\circ$ versus $\Sigma\Delta\Delta G^{\circ\prime}$ for KA and Glu binding was $p < 0.045$ and $p < 0.035$, respectively.

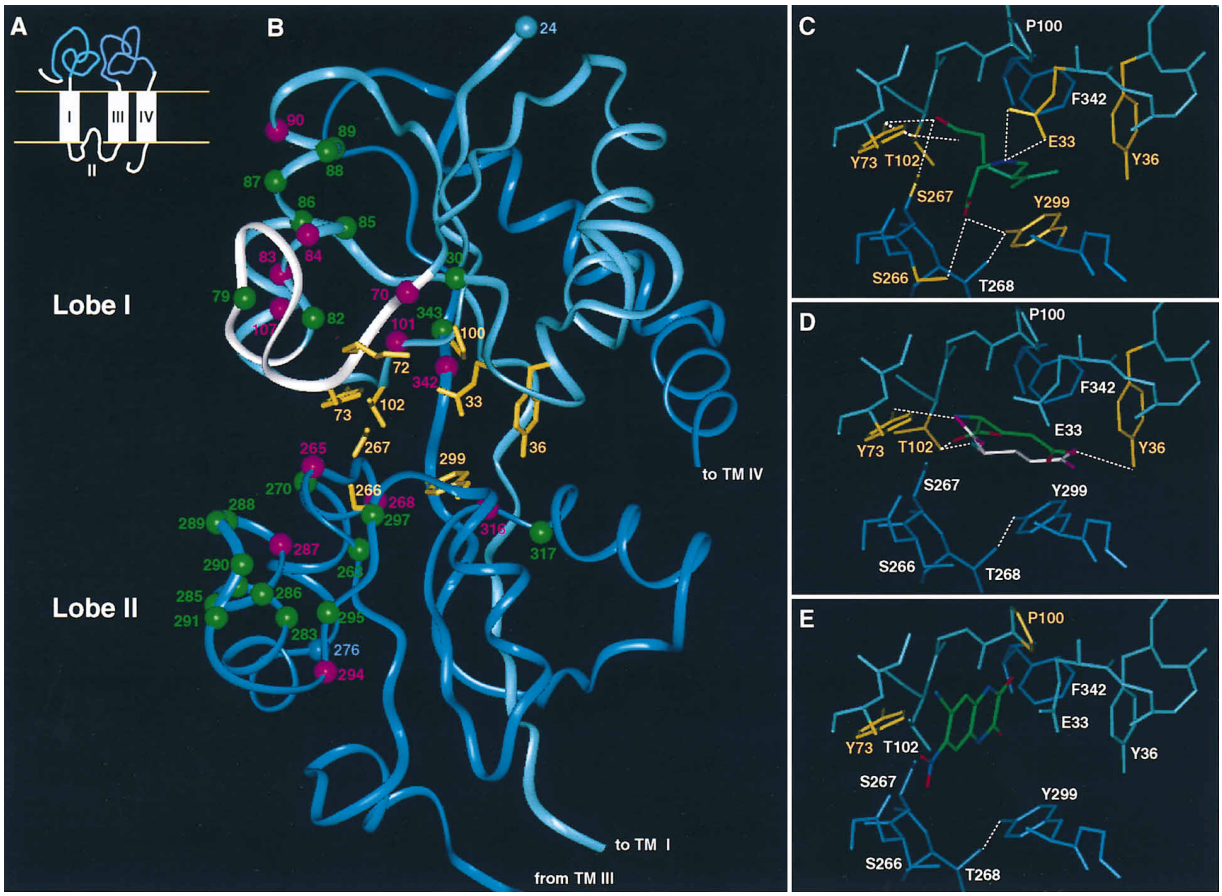


Figure 4. The KBP Hybrid Model Structure

(A) Transmembrane topology of KBP. Segment S1 (amino acids 1–147) represents the stretch extending from the first amino acid to TMI, while S2 (residues 232–397) is composed of the amino acid sequence connecting TMIII to TMIV. Segments $S'_1$ (residues 24–129) and $S'_2$ (residues 245–377), which constitute the model structure and harbor the ligand-binding pocket, are shown in cyan and blue, respectively. The white stretches show the KBP segments that were not accounted for in the model of KBP (Figure 4B). In a previous unpublished work, a KBP mutant lacking the amino-terminal first 10 amino acids was shown to bind KA as efficiently as WT KBP.

(B) The bilobated model structure of the ligand-binding domain of KBP. Segment $S'_1$, beginning at residue 24 (cyan ball), is depicted in cyan color, whereas segment $S'_2$ is shown in blue. Lobe I is built of $S'_1$ residues 24–119 and of $S'_2$ residues 341–377. Lobe II is composed of $S'_1$ residues 120–129 and $S'_2$ residues 245–340. The amino acids likely to interact with KA, Glu, and CNQX and thus to line the binding pocket are shown in yellow. These are E33, Y36, Y73, T102, S266, S267, and Y299 for KA; Y36, Y73, and T102 for Glu; Y73 and P100 for CNQX; and Y73 and K72 for GTP (Paas et al., 1996). The amino acid residues likely to be involved in stabilization of the protein tertiary structure are shown as magenta-colored balls. The amino acids shown not to be involved in ligand binding are presented as green balls. The white loop (segment G69–N81 of lobe I) is a region having no counterpart in LAOBP. It was built as described in Experimental Procedures. The blue ball at position 276 shows the beginning of the loop–$\alpha$ helix–loop–$\beta$ strand structure (amino acids 276–297; for details, see Experimental Procedures).

(C) The suggested docking mode for KA. E33 forms a hydrogen bond with the tertiary amino group of the KA ring, Y73, T102, and S267 form hydrogen bonds with the oxygen atoms of the KA 3-carboxymethyl moiety, while the hydroxyl groups of S266 and Y299 form hydrogen bonds with the KA 2-carboxyl moiety. The interaction between T268 and Y299 is equivalent to that formed in PhosBP by N177 and T141.

(D) Two docking modes for Glu are illustrated. Glu $\alpha$-carboxyl is predicted to serve as a hydrogen bond acceptor for the hydroxyl group of either Y73 or T102, while its $\alpha$-amino group interacts with the hydroxyl group of either T102 or Y73. Alternatively, a $\pi$-cation interaction between the amino group of Glu and the aromatic ring of Y73 may take place. According to both docking patterns, the Glu $\gamma$-carboxyl moiety is suggested to serve as a hydrogen bond acceptor for the hydroxyl group of Y36.

(E) Suggested docking mode of CNQX. The dashed white lines represent the possible hydrogen bonds. The ligands are shown with the following color code: carbon, green; oxygen, red; nitrogen, blue. The protein residues are colored as described in (B).

ligand-binding pocket. Yet, the R107S, T268A, E316Q, and F342I mutants did not display any KA binding though they were expressed in HEK 293 cells to very high levels and migrated on SDS–PAGE as WT KBP (Figure 3). Thus, the role of these residues in ligand binding cannot be established, since either the residues R107, T268, E316, and F342 interact directly and in a critical fashion with KA or/and play a structural role in stabilizing the conformation of the ligand-binding pocket. We favor the latter possibility, because the KBP model structure shows that R107, E316, and F342 are too far away to be in direct contact with KA, while T268 is closer but more likely to interact with S266 and Y299 (Figure 4C). It is relevant to mention that the amino acids that belong to this category are highly conserved throughout the iGluRs and KBPs.

### KBP as an Allosteric Protein

The Hill coefficient values for the displacement curves of KA observed for WT KBP and its mutants (Table 1) clearly indicate the existence of cooperative interactions between two homologous binding sites in the membranous KBP complex. The larger $n_H$ values displayed by the Y36F, Y73I, and Y299A mutants for KA binding and by Y36F and Y73I mutants for Glu binding (Table 2) are at first glance quite puzzling. However, a change in $n_H$ is expected in allosteric proteins if the transition to the high affinity state is impaired by a mutation that affects either the interconversion between states or the ability of the ligand to stabilize the high affinity state. In the case of KBP, as it is for many neurotransmitter receptors, the ligand stabilizes the transition to the high affinity state and thus the latter is likely to be affected by the mutation of a residue participating in ligand binding. Accordingly, the calculated $\Delta\Delta G^\circ$ values for the Y36F and Y73I will include a contribution to the allosteric transition, i.e., to the intersubunit interaction energy (Wyman, 1964; Levitzki, 1978). In the case of Y299A, no statistically significant difference exists between $\Delta\Delta G^\circ$ and $\Delta\Delta G^{\circ\prime}$ (see Table 3).

In view of the homology of KBP with LAOBP, it is of relevance to mention that the latter exists, in the absence of ligand, in a dynamic equilibrium of two conformations with open and closed lobes. Upon ligand binding, the closed conformation of LAOBP is being stabilized (Oh et al., 1993). If such stabilization of a closed-lobe conformation also takes place in a KBP subunit upon binding of an agonist, one may expect that the closed conformation of the neighboring subunit will be stabilized as well. Thus, mutations of some of the residues in the ligand-binding pocket are anticipated to affect the ability of the ligand to bind and regulate the allosteric transitions. Accordingly, one may suggest that, among the ligand-binding residues, Y36 and Y73 contribute to the allosteric properties of KBP, while E33, T102, S266, and S267 do not.

### A Model Structure of the Ligand-Binding Domain

The current KBP hybrid model structure of the ligand-binding domain of KBP (Figure 4A) depicts almost the entire KBP with the exception of the putative TM segments, the TMI–TMIII-connecting stretch, and the intracellularly located carboxy-terminal tail of 47 amino acids. Thus, the model includes most of the extracellularly located regions of the protein, but lacks the 18-, 13-, and 20-amino acid long extracellular segments that are respectively located adjacent to TMI, TMIII, and TMIV and that have no counterparts in the PBPs. Since segments of 13–20 amino acids can be of significant lengths, depending on their conformation, one cannot decide, as other authors did (Stern-Bach et al., 1994; Sutcliffe et al., 1996; Hirai et al., 1996), as to the parallel, perpendicular, or oblique orientation of the lobes with respect to the plane of the membrane.

Inspection of the model structure reveals several prominent structural features. First, in both lobes, a central core of a pleated sheet is found surrounded by helices. This supersecondary structure, called the Rossmann fold (Branden and Tooze, 1991), is typical not only of PBPs but also of nucleotide-binding proteins, which may account for the guanine nucleotide binding properties of KBP (Paas and Teichberg, 1992; Paas et al., 1994, 1996; Gorodinsky et al., 1993). Second, the KBP GxGxxG nucleotide binding address or glycine-rich motif (residues 69–74) is located at the opening of the interlobe cleft at an exposed position readily available for interactions with antibodies. This is in line with the observations that antibodies directed against the KBP nucleotide binding address prevent the photoaffinity-labeling reaction of GTP with KBP (Paas et al., 1996). Third, the KBP region corresponding to the flip-flop region of AMPA receptors (Sommer et al., 1990) is not located in the vicinity of the interlobe cleft but rather forms a long kinked $\alpha$-helical structure at the back of the molecule. It is depicted, in Figure 4B, as part of the dark blue segment in lobe I. It is of interest to note that mutations introduced in AMPA receptors at positions corresponding to the residues located close to the kink of this long helix were shown by Partin et al. (1995) to exert an influence on the sensitivity of GluR1 toward cyclothiazide, an agent that interferes with the desensitization process of AMPA receptors. Fourth, the residues that do not affect ligand binding (green balls in Figure 4) are located away from the ligand-binding site.

Most recently, Sutcliffe et al. (1996) have proposed a model structure of the AMPA GluR1-binding domain and a mode for KA docking in GluR6 based solely on the homology with LAOBP and on the mutations previously introduced, in GluR1, at two positions (E398 and K445) by Uchino et al. (1992) and Li et al. (1995). The proposed location of K445 in the ligand-binding pocket as proposed by Sutcliffe et al. (1996) is neither in line with our binding data nor with the results of Mano et al. (1996 and unpublished data) who did not observe changes in KA-, Glu-, and Quis-evoked responses in Xenopus oocytes injected with the GluR1 K445A mutant.

### The Specific Ligand-Binding Sites

KA interacts with all the amino acids forming the KBP ligand-binding pocket with the exception of P100. Four residues belong to the S1 region and three to the S2 region (see Figure 4A for definition and amino acid numbering), indicating that the KA-binding domain occupies the interface between the two regions. However, analysis of the contributions to the free energy of KA binding of the individual amino acid residues shows a significantly larger contribution to binding of the S1 residues (7 kcal/mol) than of the S2 residues (2.7 kcal/mol). The suggested docking modes of KA is presented in Figure 4C. It is in line with the space-filling and chemical properties of KA.

Glu interacts with three of the amino acids lining the KA-binding pocket and may bind in two docking modes, as illustrated in Figure 4D. It is of importance to note that the lobe II residues that line the ligand-binding pocket and interact with KA do not interact with Glu.

Notably, to optimize hydrogen bonding, T102 must have different side chain conformations when KA or Glu are docked within the binding pocket. In view of the homology of KBP with LAOBP, it is of relevance to mention that upon lysine binding to LAOBP, three side chains, located within the substrate binding pocket,

change their position in respect to the backbone (Figure 4b of Oh et al., 1993).

Among the residues affecting KA binding, only Y73I interacts with CNQX. The search among all the residues located in the predicted ligand-binding pocket for additional interacting residues led, following inspection of the KBP hybrid model structure, to the examination of the P100A mutant. The latter was found, indeed, to lose affinity toward CNQX. In light of the fact that none of the KA-binding residues, except for Y73, is involved in CNQX binding, and because no other residues are in suitable proximity, we suggest that CNQX docks on KBP in the vicinity of Y36 and F342. The direct interaction of these residues with CNQX could not be evaluated, since the Y36I and F342I mutants displayed no [$^3$H]KA binding activity, in line with their predicted role in stabilization of the ligand-binding pocket structure. One has also to keep in mind that CNQX may interact in part with the protein backbone.

Y73 seems to plays a crucial role in ligand recognition, as it is the only residue that interacts with KA, Glu, CNQX, as well as with guanine nucleotides (Paas et al., 1996). This residue is present in a consensus nucleotide binding address highly conserved throughout the ionotropic Glu receptor subunits that, unlike the bacterial PBPs, specifically recognize guanine derivatives in a competitive manner (Paas et al., 1996, and its references). This nucleotide binding address adopts a conformation in which the side chain of Y73 points inward into the interlobe cleft and allows its involvement in ligand binding. As a correlate, K72, which also plays a role in GTP binding (Paas et al., 1996), points away from the glutamatergic binding pocket in line with the observation that the K72A/T mutants bind KA as efficiently as WT KBP (Table 1). Computer simulation of the respective docking of KA, Glu, and CNQX in the KBP hybrid model structure clearly demonstrates that the three ligands occupy overlapping space within the ligand-binding pocket, in agreement with their competitive relationships.

The KBP model structure elaborated from this work can now hopefully serve as a template for other Glu receptors. One can expect, however, that the coordinates of model structures of the other receptors will have to be adjusted in accordance with the varying nature of the amino acid side chains that line the respective ligand-binding pocket so as to account for the diversity in the ligand binding specificities and affinities displayed by the various subtypes of Glu receptor/channels. At this stage, the KBP model structure was already used as a template for building a model of GluR1, but adjustments are needed to account for the fact that mutations that decrease KA binding to KBP affect the Glu and Quis but not the KA-induced responses of GluR1 (Mano et al., 1996).

## Experimental Procedures

### Chemicals

[Vinylidene-$^3$H]kainic acid (58 Ci/mmol) was purchased from New England Nuclear (Boston, MA). Unless stated otherwise, other chemicals were purchased from Sigma Chemical Company (St. Louis, MO).

### Preparation of KBP Mutants

KBP cDNA was subcloned in pMT3 expression vector (a gift from the Genetics Institute, Cambridge, MA) (Swick et al., 1992) between NotI and XhoI sites. Mutants were constructed by PCR with the mutagenic oligonucleotides chosen so as to introduce a new restriction site to be used for screening. For those putative mutants with the expected restriction map, the sequence was verified using the T7 sequencing kit from Pharmacia as recommended.

### Membrane Preparations and Binding Assays

Transfections of adhesive HEK 293 cells were performed as described by Paas et al. (1996). For the assay of [$^3$H]KA binding to membrane-bound WT KBP and its mutants, the protocols described by Paas et al. (1996) were used.

All binding curves were carried out at least twice with each concentration points in triplicates. Displacement curves were fitted to the equation $Y = 1 - \{[L]^n/([L]^n + [IC_{50}]^n)\}$ where Y is the fractional occupancy; [L], the concentration of the unlabeled ligand; $IC_{50}$, the concentration of the unlabeled ligand inhibiting 50% of [$^3$H]KA binding; and n being the slope factor. When a small fraction of the total ligand input (labeled and unlabeled) is bound, the free ligand concentration (total minus bound) is approximately equal to [L] and the value of the slope factor (around the $IC_{50}$) represents the Hill coefficient ($n_H$). Generally, [$^3$H]KA was added at concentrations of 50 up to 150 nM, and 0.5%–2.5% of the [$^3$H]KA input was observed as bound. The calculations of the [$^3$H]KA input concentration and that of bound [$^3$H]KA were based on the specific radioactivity and decomposition rates of [$^3$H]KA stated by the manufacturer. Values of the apparent dissociation constants for inhibition, $Ki_{app}$, were calculated from the equation: $(Ki_{app})^n = [IC_{50}]^n/\{2([I_0]/[I_1])^n - 1 + ([I_1]/Ki_{app(KA)})^n\}$ used for the case of n interacting binding sites. In the case of [$^3$H]KA displacement by KA, the equation used was $(Ki_{app})^n = [IC_{50}]^n - [I_1]/2([I_0]/[I_1])^n - 1$, where n is the Hill coefficient and $I_0$ and $I_1$ are the free [$^3$H]KA concentrations in the absence and presence of the displacer, respectively. The values for the Gibbs free energy of binding ($\Delta G^\circ$) were derived from the equation: $\Delta G^\circ = -RT \ln Ki_{app}$ where the gas constant R = 1.987 calories $\times$ degree$^{-1}$ $\times$ mole$^{-1}$ and T = 277.18 degrees for binding reactions performed at 4°C. The energies of subunit interactions ($\Delta G^\circ_H$) were calculated as described in the footnotes for Table 3 and within the text.

### Preparation of Anti-KBP Antibodies and Blotting Procedure

KBP was purified as described by Gregor et al. (1988) and injected in complete Freund's adjuvant to rabbits. The anti-KBP antibodies were affinity purified as described by Beall and Mitchell (1986). Following electrophoresis on SDS–polyacrylamide 8% slab gels, the membranous proteins were blotted to nitrocellulose paper (BA85, Schleicher and Schuell, Federal Republic of Germany) as described by Towbin et al. (1979). Detection of the immunoreactive bands was performed by using HRP-conjugated antibodies and the ECL detection reagents (Amersham International, England).

### Alignments and Computer-Assisted Molecular Modeling

The building of the model structure was based on the assumption that KBP is structurally related to the PBPs. The programs FASTA (Pearson and Lipman, 1988), BLAST (Altschul et al., 1990), and the Smith–Waterman algorithms (Smith and Waterman, 1981) were used to align separately the S1 and S2 segments of KBP (see Figure 4A for definition and amino acid numbering) with the sequences of various PBPs, including arginine-binding protein, QBP, histidine-binding protein, LAOBP, octopine-binding protein, nopaline-binding protein, and PhosBP. The three programs similarly aligned S1 with the sequences of lobe I plus the first hinge and first $\beta$ strand of lobe II in LAOBP. The resulting sequence alignments were also in general agreement with the alignment proposed by O'Hara et al. (1993), but with one significant deviation. The sequence G69–G80 instead of W82–Q92 is the insert having no corresponding sequence in LAOBP and other PBPs, in agreement with Nakanishi et al. (1990) and Cockcroft et al. (1993).

In contrast, most of the S2 segment did not show a significant amino acid sequence similarity with any PBP, in agreement with Nakanishi et al. (1990). A consensus is reached only for a short sequence located at the carboxy-terminal portion of S2 (residues 341–377), which could be aligned with the carboxy-terminal sequence of the PBPs and which forms part of lobe I.

The secondary structure predictions for the $S'_1$ and $S'_2$ segments

(see Figure 4A for definition and amino acid numbering) performed using the program PHD (Rost and Sander, 1994) showed that most of the helices, β strands, and loops were correctly identified and matched the LAOBP template. However, significant mismatches were found at two positions: the segment G69–N81 (in lobe I) was predicted to be a loop, whereas residues W82–Q92 were predicted to form an α helix, in agreement with our sequence alignment with LAOBP. Since part of the G69–N81 loop (i.e., $^{69}$GDGKYG$^{74}$) is a guanine nucleotide–binding motif in GluRs (Paas et al., 1996), its structure was constructed on the basis of the X-ray coordinates of the corresponding motif in *ras* p21 (Pai et al., 1989, 1990) and its extension $^{75}$AISPSGN$^{81}$ was built manually (white loop in Figure 4B). The second mismatch regards the structure of the chain of residues 276–297 (in lobe II). Residues 276–294 were predicted on the basis of LAOBP to form a loop–β strand–loop structure, while residues 295–297 are part of the following α helix. However, 11 amino acids of this chain have no counterpart in LAOBP (O'Hara et al., 1993; Stern-Bach et al., 1994). In contrast, the PHD program predicts for residues 276–294 a secondary structure of loop–helix–loop, whereas residues 295–297 form a β strand.

The sequence–structure compatibility of the LAOBP-based model, tested by a 3D–1D verification (Bowie et al., 1991; as implemented by Biosym Technologies), identified the mismatched segments (see above) as having erroneous folding, thus supporting our alignments and secondary structure predictions.

Looking for a solution to the folding of segment 276–297, we found that the PhosBP folds exactly as predicted for KBP by the PHD secondary structure prediction. The segment building lobe II in PhosBP is longer than the corresponding segment in LAOBP, and thus the segment K276–K297 of KBP can now be entirely aligned with specific PhosBP residues. One should note that, on the basis of the PHD secondary structure prediction, the α helix in the loop–helix–loop motif (276–294) is longer by one turn in the KBP structure model than that of the PhosBP, while the subsequent loop is shorter. Consequently, the hydrophobic residue M287 that, in strict analogy to PhosBP, was solvent accessible is not anymore in an aqueous environment. This modification is in line with the observation that substitution of M287 for the more polar alanine residue resulted in protein degradation and loss of ligand binding capability, whereas the introduction of an isofunctional side chain (valine) neither changed the ligand binding affinity nor led to protein degradation (Figure 3 and Table 1). The 3D–1D test for this hybrid model gave good scores for the whole structure.

The PhosBP is different from LAOBP not only in the folding of lobe II, but also in the relative position of its lobes. Thus, in the KBP hybrid model structure, the relative positions of the two lobes are shifted toward the PhosBP positions and now place S266, S267, and Y299 in most convenient positions to contribute to KA binding (see Figures 4B and 4C). In addition, L263, which aligns with a ligand-binding residue of LAOBP (L117), does not point into the interlobe cleft and accordingly is unlikely to interact with KA, as indeed observed.

## Acknowledgments

Correspondence should be addressed to V. I. T. or A. D.-T. We are indebted to Prof. J.-P. Changeux for his unfailing support and judicious advice and Dr. G. Schreiber for useful discussions. We thank Mrs. C. Lamed for technical assistance. This work was supported by grants to V. I. T from the Minerva Foundation (Munich, Federal Republic of Germany), The Golden Charitable Trust, and the Leo and Julia Forchheimer Center for Molecular Genetics. A. D.-T. and F. M. were supported by grants from the College de France, Centre National de la Recherche Scientifique, the Association Francaise Contre les Myopathies, the Human Frontier Science Program, and the European Economic Community Biotech Program. M. E. and V. I. T. acknowledge the support of the Kimmelman Center for Biomolecular Assembly. V. I. T. holds the Louis and Florence Katz-Cohen professorial chair of Neuropharmacology.

The costs of publication of this article were defrayed in part by the payment of page charges. This article must therefore be hereby marked *"advertisement"* in accordance with 18 USC Section 1734 solely to indicate this fact.

Received July 29, 1996; revised September 16, 1996.

## References

Altschul, S.F., Gish, W., Miller, W., Myers, E.W., and Lipman, D.J. (1990). Basic local alignment search tool. J. Mol. Biol. *215*, 403–410.

Ames, G.F.-L. (1986). Bacterial periplasmic transport system: structure, mechanism and evolution. Annu. Rev. Biochem. *55*, 397–425.

Beall, J.A., and Mitchell, G.F. (1986). Identification of a particular antigen from a parasite cDNA library using antibodies affinity purified from selected proteins of Western blots. J. Immunol. Meth. *86*, 217–223.

Bennett, J.A., and Dingledine, R. (1995). Topology profile for a glutamate receptor: three transmembrane domains and a channel-lining reentrant membrane loop. Neuron *14*, 373–384.

Berland, C.R., Sigurskjold, B.W., Stoffer, B., Frandsen, T.P., and Svensson, B. (1995). Thermodynamics of inhibitor binding to mutant forms of glucoamylase from *Aspergillus niger* determined by isothermal titration calorimetry. Biochemistry *34*, 10153–10161.

Bourne, H.R., Sanders, D.A., and McCormick, F. (1991). The GTPase superfamily: conserved structure and molecular mechanism. Nature *349*, 117–127.

Bowie, J.U., Luthy, R., and Eisenberg, D. (1991). A method to identify protein sequences that fold into a known three-dimensional structure. Science *253*, 164–170.

Branden, C., and Tooze, J. (1991). Introduction to Protein Structure (London: Garland Publishing, Incorporated).

Cockcroft, V.B., Ortells, M.O., Thomas, P., and Lunt, G.G. (1993). Homologies and disparities of glutamate receptors: a critical analysis. Neurochem. Int. *23*, 583–594.

Gasic, G.P., and Hollmann M. (1992). Molecular neurobiology of glutamate receptors. Annu. Rev. Physiol. *54*, 507–536.

Gorodinsky, A., Paas, Y., and Teichberg, V.I. (1993). A ligand binding study of the interactions of guanine nucleotides with non-NMDA receptors. Neurochem. Int. *23*, 285–291.

Gregor, P., Eshhar, N., Ortega, A., and Teichberg, V.I. (1988). Isolation, immunochemical characterization and localization of the kainate sub-class of glutamate receptor from chick cerebellum. EMBO J. *7*, 2673–2679.

Gregor, P., Mano, I., Maoz, I., McKeown, M., and Teichberg, V.I. (1989). Molecular structure of the chick cerebellar kainate binding subunit of a putative glutamate receptor. Nature *342*, 689–692.

Hanks, S.K., Quinn, A.-M., and Hunter, T. (1988). The protein kinase family: conserved features and deduced phylogeny of catalytic domains. Science *241*, 42–52.

Hirai, H., Kirsch, J., Laube, B., Betz, H., and Kuhse, J. (1996). The glycine binding site of the N-methyl-D-aspartate receptor subunit NR1: identification of novel determinants of co-agonist potentiation in the extracellular M3–M4 loop region. Proc. Natl. Acad. Sci. USA *93*, 6031–6036.

Hollmann, M., and Heinemann, S. (1994). Cloned glutamate receptors. Annu. Rev. Neurosci. *17*, 31–108.

Hollmann, M., Maron, C., and Heinemann, S. (1994). N-glycosylation site tagging suggests a three transmembrane domain topology for the glutamate receptor GluR1. Neuron *13*, 1331–1343.

Kang, C.-H., Shin, W.-C., Yamagata, Y., Gokcen, S., Ames, G.F.-L., and Kim, S.-H. (1991). Crystal structure of the lysine-, arginine-, ornithine-binding protein (LAO) from *Salmonella typhimurium* at 2.7-Å resolution. J. Biol. Chem. *266*, 23893–23899.

Kuryatov, A., Laube, B., Betz, H., and Kuhse, J. (1994). Mutational analysis of the glycine-binding site of the NMDA receptor: structure similarity with bacterial amino acid–binding proteins. Neuron *12*, 1291–1300.

Kuusinen, A., Arvola, M., and Keinänen, K. (1995). Molecular dissection of the agonist binding site of an AMPA receptor. EMBO J. *14*, 6327–6332.

Levitzki, A. (1978). Quantitative Aspects of Allosteric Mechanism (Berlin: Springer-Verlag).

Li, F., Owens, N., and Verdoorn, T.A. (1995). Functional effects of mutations in the putative agonist binding region of recombinant α-amino-3-hydroxy-5-methyl-4-isoxazolepropionic acid receptors. Mol. Pharmacol. *47*, 148–154.

Luecke, H., and Quiocho, F. (1990). High specificity of a phosphate transport protein determined by hydrogen bonds. Nature *347*, 402–406.

Mano, I., Lamed, Y., and Teichberg, V.I. (1996). A venus flytrap mechanism for activation and desensitization of α-amino-3-hydroxy-5-methyl-4-isoxazole propionic acid receptors. J. Biol. Chem. *271*, 15299–15302.

Nakanishi, N., Shneider, N.A., and Axel, R. (1990). A family of glutamate receptor genes: evidence for the formation of heteromultimeric receptors with distinct channel properties. Neuron *5*, 569–581.

Oh, B.-H., Pandit, J., Kang, C.-H., Nikaido, K., Gokcen, S., Ames, G.F.-L., and Kim, S.-H. (1993). Three-dimensional structure of the periplasmic lysine/arginine/ornithine-binding protein with and without a ligand. J. Biol. Chem. *268*, 11348–11355.

Oh, B.-H., Kang, C.-H., De Bondt, H., Kim, S.-H., Nikaido, K., Joshi, A.K.S., and Ames, G.F.-L. (1994). The bacterial periplasmic histidine-binding protein: structure/function analysis of the ligand-binding site and comparison with related proteins. J. Biol. Chem. *269*, 4135–4143.

O'Hara, P.J., Sheppard, P.O., Thφgersen, H., Venezia, D., Haldeman, B.A., McGrane, V., Houamed, K.M., Thomsen, C., Gilbert, T.L., and Mulvihill, E.R. (1993). The ligand-binding domain in metabotropic glutamate receptors is related to bacterial periplasmic binding proteins. Neuron *11*, 41–52.

Paas, Y., and Teichberg, V.I. (1992). The ligand binding site of the chick cerebellar glial kainate receptor. Int. J. Dev. Neurosci. *10* (Suppl. 1), 47.

Paas, Y., Devillers-Thiéry, A., Changeux, J.-P., Maoz, I., and Teichberg, V.I. (1994). The guanine nucleotide binding site of the chick cerebellar kainate binding protein and its relevance to the ligand binding site of glutamate receptors. J. Neurochem. *63* (Suppl. 1), S1D.

Paas, Y., Devillers-Thiéry, A., Changeux, J.-P., Medevielle, F., and Teichberg, V.I. (1996). Identification of an extracellular motif involved in the binding of guanine nucleotides by a glutamate receptor. EMBO J. *15*, 1548–1556.

Pai, E.F., Kabsch, W., Krengel, U., Holmes, K.C., John, J., and Wittinghofer, A. (1989). Structure of the guanine-nucleotide-binding domain of the Ha-*ras* oncogene product p21 in the triphosphate conformation. Nature *341*, 209–214.

Pai, E.F., Krengel, U., Petsko, G.A., Goody, R.S., Kabsch, W., and Wittinghofer, A. (1990). Refined crystal structure of the triphosphate conformation of H-ras p21 at 1.35 Å resolution: implications for the mechanism of GTP hydrolysis. EMBO J. *9*, 2351–2359.

Partin, K.M., Bowie, D., and Mayer, M.L. (1995). Structural determinants of allosteric regulation in alternatively spliced AMPA receptors. Neuron *14*, 833–843.

Pearson, W.R., and Lipman, D.J. (1988). Improved tools for biological sequence comparison. Proc. Natl. Acad. Sci. USA *85*, 2444–2448.

Pin, J.P., and Duvoisin, R. (1995). The metabotropic glutamate receptors: structure and functions. Neuropharmacology *34*, 1–26.

Quiocho, F.A. (1990). Atomic structures of periplasmic binding proteins and the high-affinity active transport system in bacteria. Phil. Trans. Roy. Soc. (Lond.) B *326*, 341–351.

Rost, B., and Sander, C. (1994). Combining evolutionary information and neural networks to predict protein secondary structure. Proteins *19*, 55–72.

Schreiber, G., and Fersht, A.R. (1995). Energetics of protein–protein interactions: analysis of the Barnase–Barstar interface by single mutations and double mutant cycles. J. Mol. Biol. *248*, 478–486.

Smith, T.F., and Waterman, M.S. (1981). Identification of common molecular subsequences. J. Mol. Biol. *147*, 195–197.

Sommer, B., Keinänen, K., Verdoorn, T.A., Wisden, W., Burnashev, N., Herb, A., Köhler, M., Takagi, T., Sakmann, B., and Seeburg, P.H. (1990). Flip and flop: a cell-specific functional switch in glutamate-operated channels of the CNS. Science *249*, 1580–1585.

Stern-Bach, Y., Bettler, B., Hartley, M., Sheppard, P.O., O'Hara, P.J., and Heinemann, S.F. (1994). Agonist selectivity of glutamate receptors is specified by two domains structurally related to bacterial amino acid–binding proteins. Neuron *13*, 1345–1357.

Sutcliffe, M.J., Wo, Z.G., and Oswald, R.E. (1996). Three-dimensional models of non-NMDA glutamate receptors. Biophys. J. *70*, 1575–1589.

Swick, A.G., Janicot, T., Cheneval-Kastelic, T., McLenithan, J.C., and Lane, M.D. (1992). Promoter-cDNA-directed heterologous protein expression in *Xenopus laevis* oocytes. Proc. Natl. Acad. Sci. USA *89*, 1812–1816.

Towbin, H., Staehelin, T., and Gordon, J. (1979). Electrophoretic transfer of proteins from polyacrylamide gels to nitrocellulose sheets: procedure and some applications. Proc. Natl. Acad. Sci. USA *76*, 4350–4354.

Uchino, S., Sakimura, K., Nagahari, K., and Mishina, M. (1992). Mutations in a putative agonist binding region of the AMPA-selective glutamate receptor channel. FEBS Lett. *308*, 253–257.

Wada, K., Dechesne, C.J., Shimasaki, S., King, R.G., Kusano, K., Buonanno, A., Hampson, D.R., Banner, C., Wenthold, R.J., and Nakatani, Y. (1989). Sequence and expression of a frog brain complementary DNA encoding a kainate-binding protein. Nature *342*, 684–688.

Wafford, K.A., Kathoria, M., Bain, C.J., Marshall, B., Le Bourdelles, B., Kemp, J.A., and Whiting, P.J. (1995). Identification of amino acids in the N-methyl-D-aspartate receptor NR1 subunit that contribute to the glycine binding site. Mol. Pharmacol. *47*, 374–380.

Wang, Z., Choudhary, A., Ledvina, P.S., and Quiocho, F.A. (1994). Fine tuning the specificity of the periplasmic phosphate transport receptor. J. Biol. Chem. *269*, 25091–25094.

Wo, Z.G., and Oswald, R.E. (1994). Transmembrane topology of two kainate receptor subunits revealed by N-glycosylation. Proc. Natl. Acad. Sci. USA *91*, 7154–7158.

Wo, Z.G., and Oswald, R.E. (1995). A topological analysis of goldfish kainate receptors predicts three transmembrane segments. J. Biol. Chem. *270*, 2000–2009.

Wyman, J., Jr. (1964). Linked functions and reciprocal effects in hemoglobin: a second look. Adv. Prot. Chem. *19*, 223–286.